AIP | Applied Physics Letters

Electronic transport in highly conducting Si-doped ZnO thin films prepared by pulsed laser deposition

Vladimir L. Kuznetsov, Alex T. Vai, Malek Al-Mamouri, J. Stuart Abell, Michael Pepper, and Peter P. Edwards

Citation: Applied Physics Letters **107**, 232103 (2015); doi: 10.1063/1.4936613
View online: http://dx.doi.org/10.1063/1.4936613
View Table of Contents: http://scitation.aip.org/content/aip/journal/apl/107/23?ver=pdfcov
Published by the AIP Publishing

Electronic transport in highly conducting Si-doped ZnO thin films prepared by pulsed laser deposition

Vladimir L. Kuznetsov,[1] Alex T. Vai,[1] Malek Al-Mamouri,[2] J. Stuart Abell,[2] Michael Pepper,[3] and Peter P. Edwards[1,a)]
[1]*Department of Chemistry, Inorganic Chemistry Laboratory, University of Oxford, Oxford OX1 3QR, United Kingdom*
[2]*Department of Metallurgy and Materials, University of Birmingham, Birmingham B15 2TT, United Kingdom*
[3]*Department of Electronic and Electrical Engineering, University College London, London WC1E 7JE, United Kingdom*

(Received 11 August 2015; accepted 15 November 2015; published online 8 December 2015)

Highly conducting ($\rho = 3.9 \times 10^{-4}\,\Omega$cm) and transparent (83%) polycrystalline Si-doped ZnO (SiZO) thin films have been deposited onto borosilicate glass substrates by pulsed laser deposition from $(ZnO)_{1-x}(SiO_2)_x$ ($0 \le x \le 0.05$) ceramic targets prepared using a sol-gel technique. Along with their structural, chemical, and optical properties, the electronic transport within these SiZO samples has been investigated as a function of silicon doping level and temperature. Measurements made between 80 and 350 K reveal an almost temperature-independent carrier concentration consistent with degenerate metallic conduction in all of these samples. The temperature-dependent Hall mobility has been modeled by considering the varying contribution of grain boundary and electron-phonon scattering in samples with different nominal silicon concentrations. © *2015 AIP Publishing LLC*. [http://dx.doi.org/10.1063/1.4936613]

Transparent conducting oxides (TCOs) are widely employed as transparent electrodes in photovoltaic cells, flat panel and touch screen displays, light emitting diodes, and low-emittance window coatings.[1,2] Tin-doped indium oxide (ITO) is currently the most widely used TCO material for high-end applications because it possesses a remarkable combination of low electrical resistivity and high transparency to visible light. However, the high cost, price volatility, and scarcity of indium are all factors limiting the growth of macroelectronics, which include large-area, cost sensitive devices like solar panels, large displays, electronic paper, and solid-state lighting. Much research has therefore been aimed at producing indium-free or reduced indium TCO materials for these types of applications.[3,4]

As an abundant and non-toxic TCO material, doped zinc oxide has been the subject of considerable research interest and has been utilized in numerous TCO applications.[5] In particular, ZnO doped with silicon (SiZO) has attracted a great deal of recent attention.[6–9] Not only has Si been found to be an effective *n*-type dopant, it is expected to act as a two electron donor when substituted for Zn in the ZnO lattice and could thus potentially generate higher free carrier densities at a given doping level than the one-electron Group 13 dopants Al, Ga, or In.[10]

Several deposition techniques have previously been utilized to produce SiZO thin films, including RF magnetron sputtering,[6,11] pulsed laser deposition,[8,12,13] sol-gel spin coating,[14] atomic layer deposition,[15] and spray pyrolysis.[9,16] An electrical resistivity as low as $3.8 \times 10^{-4}\,\Omega$cm with an average transmittance of 85% in the visible region has been reported for SiZO thin films deposited at a substrate temperature of 250 °C by RF magnetron sputtering.[6] Recently, we also reported on fluoride-enhanced silicon doping of ZnO thin films prepared by spray pyrolysis, which achieved electrical resistivity as low as $1.5 \times 10^{-3}\,\Omega$cm and a transparency of 87% without any additional post-deposition treatment.[16] These results demonstrate the potential of SiZO as an entirely earth-abundant, low-cost substitute for ITO. However, there is still limited information in the literature concerning the fundamental factors that determine the composition (i.e., doping) dependence of optoelectronic properties in SiZO thin films.

In this letter, we report on a series of SiZO thin films prepared by pulsed laser deposition from ceramic targets having Si concentrations in the range of 0–5 at. %. Further details of target preparation and the deposition procedure are available in the supplementary material.[17] The Hall effect and resistivity of the samples were measured between 80 and 350 K to better understand how varying silicon content affects electrical transport phenomena in these polycrystalline films. X-ray diffraction analysis showed that all films only exhibit diffraction peaks corresponding to the (002) and (004) planes of ZnO in the wurtzite structure, indicating a strong preference for crystallites in the samples to be oriented with their *c*-axis perpendicular to the substrate.[17] Within experimental error, the position and breadth of the Bragg peaks remains constant upon addition of Si; this can be attributed to the very similar covalent radii of Zn and Si (118 and 116 pm, respectively).[18] While the precise silicon doping level in deposited thin films can deviate somewhat from the nominal doping level of the target, EDX and XPS analyses on several samples clearly show the progressively higher silicon incorporation into the samples with increasing

a)Author to whom correspondence should be addressed. Electronic mail: peter.edwards@chem.ox.ac.uk

nominal doping levels.[17] For clarity, samples will be referred to using the nominal doping level in the results and discussion that follow.

The room temperature electrical transport properties of SiZO thin films are summarized in Figure 1. Both the carrier concentration and carrier mobility initially increase with increasing Si doping and reach maximum values of $6.0 \times 10^{20}\,\mathrm{cm}^{-3}$ and $27\,\mathrm{cm}^2\mathrm{V}^{-1}\mathrm{s}^{-1}$, respectively, at a nominal doping level of 2 at. % Si. Since in the free electron picture, resistivity is inversely proportional to carrier concentration and mobility via $1/\rho = \sigma = \mathrm{ne}\mu$, this is also the sample having the lowest electrical resistivity of $3.9 \times 10^{-4}\,\Omega\mathrm{cm}$. The rise in electron density with increasing silicon content is consistent with the fact that Si is an effective *n*-type dopant in ZnO and that Si doping, rather than induced changes in oxygen stoichiometry, is responsible for the changes in electrical properties. This is also reasonable given that the atmosphere was kept at the same oxygen partial pressure (2 mTorr) for each deposition run.

At Si concentrations above 2 at. %, both the carrier concentration and mobility decrease with the further addition of silicon, indicating that additional dopant atoms are no longer leading to net charge carrier generation. Previous reports on SiZO films,[9,12,13] as well as on some ZnO films doped with Group 13 elements,[19,20] have also shown that electrical properties are maximized at doping levels between 2 and 3 at. %.

The temperature dependences of resistivity, carrier concentration, and carrier mobility in undoped and SiZO thin films with different Si contents are presented in Figure 2 over the range of 80–350 K. For all samples, the carrier concentration is practically independent of temperature, implying that the films are degenerate semiconductors with the

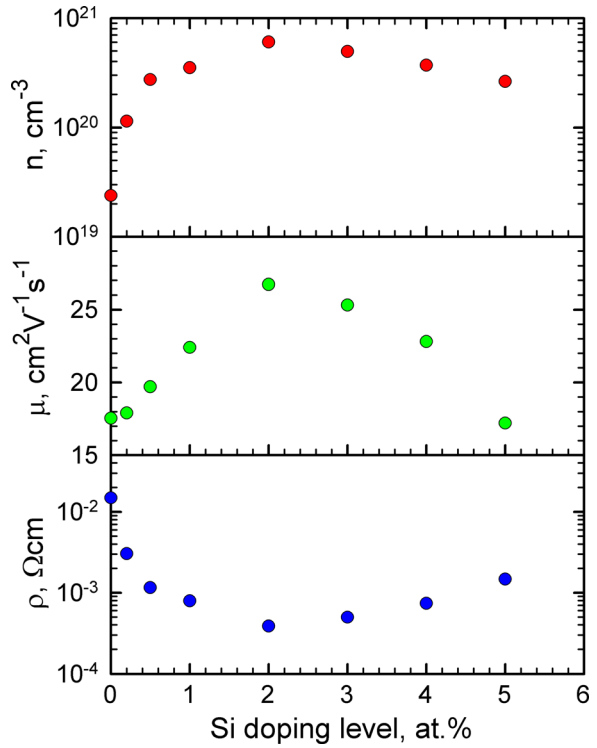

FIG. 1. Room-temperature variations of electron concentration (n), mobility (μ), and electrical resistivity (ρ) of Si-doped ZnO thin films as a function of nominal silicon doping level.

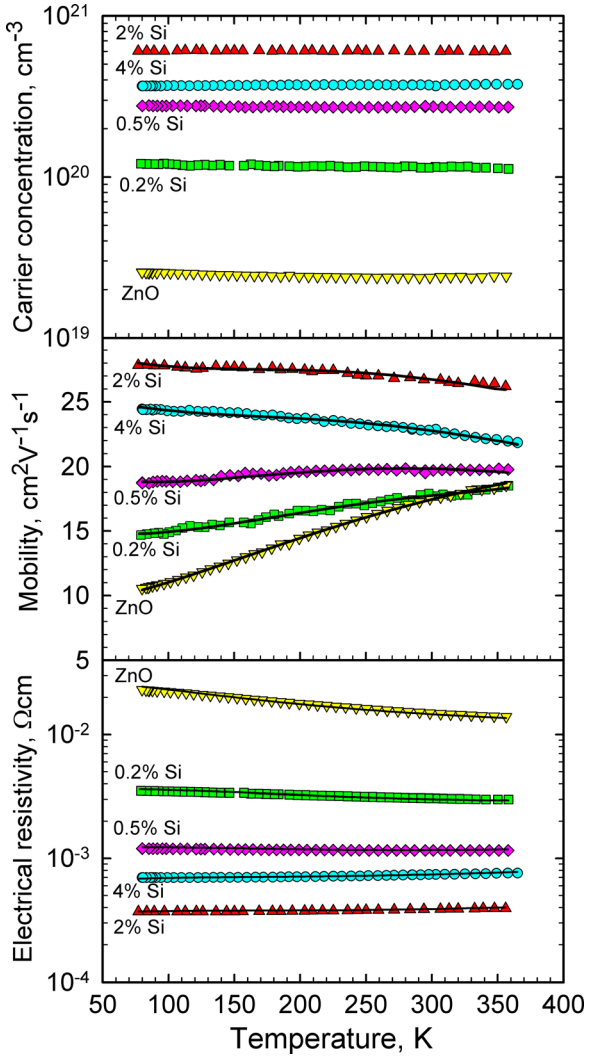

FIG. 2. Temperature dependence of carrier concentration, carrier mobility, and electrical resistivity of undoped and silicon-doped ZnO thin films with different nominal Si concentrations. The solid lines show theoretical temperature dependence of mobility and electrical resistivity based upon a model accounting for the effects of grain boundary and acoustic phonon scattering (Equation 3).

Fermi level located above the conduction band minimum. This is consistent with the fact that even the nominally undoped film has a carrier density higher than the Mott critical concentration of $6.4 \times 10^{18}\,\mathrm{cm}^{-3}$ anticipated for the metal-insulator transition in ZnO.[9,21] This also implies that changes in sample resistivity with temperature are almost entirely driven by changes in carrier mobility.

For samples with a nominal doping level of 2% or greater, the carrier mobility decreases with increasing temperature, while films with a Si content of 0.5% or below show the opposite slope (Figure 2, middle).

A representative set of SiZO optical transmission spectra is shown in Figure 3. The average transmittance of these samples to visible wavelengths (400–750 nm) ranged from 75% to 83%, with the 2 at. % Si-doped ZnO film having the highest value. A decrease in optical transmission in the near IR region (750–2500 nm) occurs as increasing carrier concentration up to 2 at. % Si leads to a blueshift of the conduction electron plasma frequency. This trend reverses as the

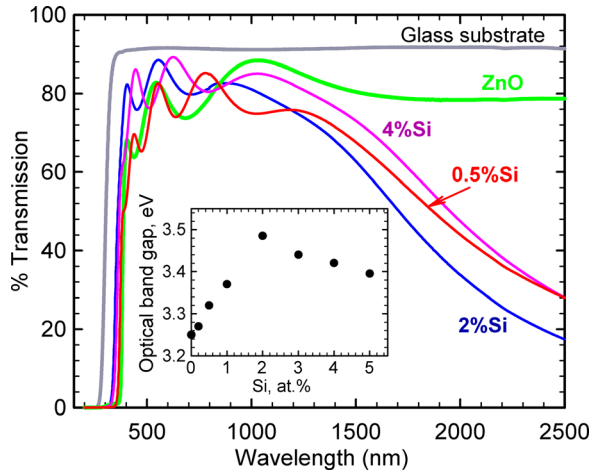

FIG. 3. Optical transmission data for SiZO thin films with different dopant concentrations. The inset displays ZnO optical bandgap energy calculated using the Tauc relation as a function of nominal Si concentration.

carrier concentration decreases in films with a higher nominal silicon content.

Likewise, increases in carrier concentration also lead to a Burstein-Moss blueshift of the ZnO optical bandgap transition in the UV region. This is clearly observed by using the Tauc relation to calculate the direct optical bandgap energies (Figure 3, inset), which show changes that correlate well with the variations in carrier concentration.

In analyzing the macroscopic electrical performance of these SiZO samples (and doped TCOs in general), two key factors arise. The first is the influence of extrinsic dopants on the concentration and mobility of free carriers. The second is that such films are almost invariably polycrystalline, which means that electronic conduction may be governed not only by the properties of grain interiors but also by those of the grain boundaries between them.

A number of theoretical studies have been performed on the formation of native and extrinsic dopant defects in ZnO as a function of Fermi energy.[10,22,23] Such works show that substitution at tetrahedral zinc sites or being located at octahedral interstitial positions are the two most energetically plausible states for cationic dopants in ZnO.[23–26] These studies also suggest that the lower formation energy of substitutional defects favors their formation over that of interstitial defects at low dopant concentrations.[23] However, as the total concentration of impurities increases, a solubility limit for dopant incorporation at substitutional sites will be eventually reached, meaning that further impurities will increasingly reside at interstitial sites and perhaps eventually precipitate as secondary phases.

Unlike cationic dopants at substitutional sites which are shallow donors and from which conduction electrons are easily freed, for example, via $Si_{Zn}^{2+} \rightarrow Si_{Zn}^{4+} + 2e^{-}$, interstitial defects generally form donor states that are too deep in the ZnO band gap to effectively contribute conduction electrons at room temperature.[24] At the same time, interstitial defects can still act as scattering centers and reduce carrier mobility. Such a picture would be consistent with our experimental data if the thermodynamic limit for the concentration of substitutional silicon defects is ~2 at. % Si. In this case, further addition of silicon beyond 2 at. % would result mostly in formation of interstitial defects that do not contribute to further increases in carrier concentration, but do lead to a decrease in carrier mobility (Figure 1).

Another plausible mechanism for the plateau in carrier concentration is the compensatory formation of intrinsic acceptor defects. For instance, a recently published DFT study found that an increasing electron chemical potential due to Si doping leads to spontaneous localization of electrons by[10]

$$Zn^{2+} + 2e^{-} \rightleftarrows Zn^{0} \rightleftarrows V_{Zn} + Zn_{i}^{0}. \quad (1)$$

Wang *et al*. have shown experimentally that in electron-rich ZnO, the resulting reduced, interstitial Zn^{0}_{i} can be stabilized by interaction with lattice Zn^{2+} to form $(Zn_2)^{2+}$ dimeric states.[27] The formation of such defects would also contribute to carrier scattering and a reduction in mobility, while at the same time localizing electrons and causing carrier concentration to stabilize at a limiting value. Owing to differences between nominal and actual film doping levels, these models should be taken as qualitative explanations for decreasing doping efficiency with increasing silicon concentration. Additional work to characterize the local structure around defects in these samples and more quantitative chemical analysis will be needed to determine the relative contribution of these two mechanisms at various silicon concentrations.

For nominal doping levels of less than 2 at. % Si, Figure 1 also shows that the carrier mobility in SiZO films increases with Si doping in concert with carrier concentration. Notably, the undoped ZnO thin film displays the lowest mobility of the samples in this series. Furthermore, Figure 2 shows that the carrier mobility of heavily doped films ($\geq$2 at. % Si) decreases with increasing temperature, while lightly doped films exhibit a thermally activated mobility. These trends are clearly inconsistent with a situation where impurities are the dominant cause of carrier scattering and must instead arise from the polycrystalline nature of the samples.

Grain boundaries in ZnO are disordered regions which tend to be oxygen-rich and hence dominated by defects that can trap free electrons from nearby grain interiors. This results in local depletion of carrier electrons from the bulk and a buildup of negative charge at grain boundaries, leading to the formation of a potential barrier between the grains that can inhibit electronic transport.[28–30] Another example of a grain boundary effect is the preferential migration of impurity atoms to grain boundaries, which can also lead to the development of potential barriers. This has been exploited to great effect in the production of ZnO-based varistors with non-linear I-V characteristics,[28,31] and has also been predicted by DFT analysis for silicon impurities in ZnO.[10] Our XPS results also indicate a surface enrichment of silicon in these samples that can also be explained by impurity segregation.[17]

The extent to which the grain boundary effects limit carrier transport is related to the height of the boundary potential barrier relative to the Fermi level E_F. For a constant barrier height, raising E_F by increasing carrier concentration or temperature makes the potential barrier increasingly insignificant to electrical transport, as an increasing proportion of

free electrons have enough energy to surmount the barrier without the need for quantum tunneling. Therefore, an increased mobility with increasing carrier concentration can be explained by invoking the interplay of grain boundary scattering and changes in carrier concentration with doping.

Generalizing the earlier work of Seto, and Orton and Powell,[32,33] Prins *et al*. have derived a model for grain-boundary limited carrier mobility (μ_{gb}) valid for both degenerate and non-degenerate semiconductors

$$\mu_{gb}(T) = BT \ln\left[1 + \exp\left(-\frac{\Phi}{k_B T}\right)\right], \quad (2)$$

where B is a parameter which depends on the carrier concentration, the effective electron mass, the grain size, the carrier mean free path and the width of the potential barrier. k_B is the Boltzmann constant, and Φ is the energy of the top of the average grain boundary potential barrier relative to the Fermi level within the grain.[34] For a temperature-independent carrier concentration (as is the case here, Figure 2, top), B is also temperature-independent.

Grain boundary scattering cannot account for the decrease in carrier mobility with increasing temperature observed for SiZO samples with high ($\geq$2 at. %) silicon concentrations (Figure 2, middle). A number of scattering mechanisms with different temperature dependences are possible within the interiors of ZnO grains, including acoustic phonon, polar optical phonon, and piezoelectric mode scattering.[35] From a preliminary fitting of experimental results, acoustic phonon scattering was found to dominate over other phonon-carrier modes for all samples in the temperature ranges studied, allowing the effect of phonon scattering on carrier mobility to be satisfactorily approximated as $\mu_{ph} \propto T^{-3/2}$.[36] By assuming that grain boundary and acoustic phonon scattering mechanisms act independently, their combined effects on mobility can be described using Matthiessen's rule, leading to a model for a temperature-dependent mobility $\mu_{tot}(T)$

$$\mu_{tot}(T) = \left(\frac{1}{BT \ln\left[1 + \exp\left(-\frac{\Phi}{k_B T}\right)\right]} + \frac{1}{AT^{-3/2}}\right)^{-1}, \quad (3)$$

where A, B, and Φ are the parameters to be fit. The best fit values for these parameters are summarized in Table I, with the corresponding temperature-dependent mobility and resistivity based on this model shown in Figure 2 as solid lines.

TABLE I. Parameters resulting from fitting of variable temperature Hall mobility data from SiZO thin films of various carrier concentrations using Equation (3).

Nominal doping, at. % Si	n, 10^{20} cm^{-3}	Φ, meV	A, 10^5 cm^2/(V s K$^{3/2}$)	B, 10^{-2} cm^2/Vs
0	0.24	−11.9	7.53	6.96
0.2	1.12	−20.0	5.30	6.05
0.5	2.73	−22.5	3.90	7.35
2	5.93	−25.8	4.60	9.76
4	3.57	−24.9	3.72	8.36

The derived values of Φ are negative for all samples, indicating that E_F is higher than the top of the average grain boundary potential barrier in each case. Importantly, this is independent corroboration that all of the samples are degenerate conductors, as previously inferred from observation of a temperature-independent carrier concentration (Figure 2, top).

The fact that mobility still shows a positive temperature dependence for the lower carrier concentration samples, despite the Fermi level being higher than the grain boundary barrier, may be understood by noting that *all* free carriers within the grains of a polycrystalline material will contribute to the measured Hall voltage and hence carrier concentration, including those that cannot freely participate in *inter*-grain electronic conduction due to grain boundary potential barriers. In contrast, the corresponding direct current conductivity σ only measures carriers with enough energy to participate in *inter*-grain conduction.[37] For the free-electron description $\sigma = ne\mu$ to still hold, the *inter*-grain Hall mobility must be lower than the *intra*-grain mobility by a factor related to the proportion of total carriers that are trapped within grains. Thus, when thermal energy can excite carriers from states with energies below the top of the grain boundary barrier to those above, the fraction of charge carriers free to participate in inter-grain conduction, and hence the Hall mobility, can be thermally activated. This is the situation observed for ZnO samples doped with 0.5 at. % Si and below. For samples with higher carrier concentrations, the Fermi level sits so far above (more than kT above) the top of the average grain boundary potential barrier that the barriers become insignificant, clearly revealing the decreasing mobility with increasing temperature expected for metallic conduction when intra-grain processes such as electron-phonon scattering dominate.

We have shown that Si acts as an effective donor impurity in ZnO thin films prepared by PLD up to about 2 at. % Si. As the silicon content of the films increases further, the carrier concentration plateaus while the carrier mobility continues to fall. This can be explained by the increasing incorporation of Si at electrically inactive interstitial sites or by the spontaneous formation of intrinsic compensating defects that can still act as scattering centers. Consistent with degenerate conduction, the carrier concentration for each SiZO film is practically temperature independent. The experimental temperature dependence of carrier mobility in SiZO can be effectively modeled by considering jointly carrier-phonon scattering within the grains and grain boundary potential barriers, whose influence on electronic transport changes as a function of carrier concentration.

The authors thank Mr. A. Bradshaw for technical assistance with the PLD facilities at the Department of Metallurgy and Materials, University of Birmingham and also acknowledge the EPSRC for funding these PLD facilities. The authors also gratefully acknowledge support from the EPSRC IAA scheme and Dr. A. Barlow for the collection of X-ray photoelectron spectra at the National EPSRC XPS Users' Service (NEXUS) at Newcastle University, an EPSRC Mid-Range Facility.

[1]D. Ginley, H. Hosono, and D. C. Paine, *Handbook of Transparent Conductors* (Springer, New York, 2011).
[2]C. F. Klingshirn, A. Waag, A. Hoffmann, and J. Geurts, *Zinc Oxide: From Fundamental Properties Towards Novel Applications* (Springer, Heidelberg, Germany, 2010).
[3]T. Minami, MRS Bull. **25**, 38 (2000).
[4]T. Minami, Thin Solid Films **516**, 5822 (2008).
[5]H. Morkoç and Ü. Özgür, *Zinc Oxide: Fundamentals, Materials and Device Technology* (Wiley-VCH, Weinheim, Germany, 2009).
[6]T. Minami, H. Sato, H. Nanto, and S. Takata, Jpn. J. Appl. Phys., Part 2 **25**, L776 (1986).
[7]A. K. Das, P. Misra, and L. M. Kukreja, J. Phys. D: Appl. Phys. **42**, 165405 (2009).
[8]J. Clatot, G. Campet, A. Zeinert, C. Labrugère, M. Nistor, and A. Rougier, Sol. Energy Mater. Sol. Cells **95**, 2357 (2011).
[9]N. Rashidi, V. L. Kuznetsov, J. R. Dilworth, M. Pepper, P. J. Dobson, and P. P. Edwards, J. Mater. Chem. C **1**, 6960 (2013).
[10]W. Körner and C. Elsässer, Phys. Rev. B **83**, 205306 (2011).
[11]R. E. Treharne, L. J. Phillips, K. Durose, A. Weerakkody, I. Z. Mitrovic, and S. Hall, J. Appl. Phys. **115**, 063505 (2014).
[12]A. K. Das, R. S. Ajimsha, and L. M. Kukreja, Appl. Phys. Lett. **104**, 042112 (2014).
[13]J. Clatot, M. Nistor, and A. Rougier, Thin Solid Films **531**, 197 (2013).
[14]I. Sorar, D. Saygin-Hinczewski, M. Hinczewski, and F. Z. Tepehan, Appl. Surf. Sci. **257**, 7343 (2011).
[15]H. Yuan, J. Mater. Sci.: Mater. Electron. **23**, 2075 (2012).
[16]N. Rashidi, A. T. Vai, V. L. Kuznetsov, J. R. Dilworth, and P. P. Edwards, Chem. Commun. **51**, 9280 (2015).
[17]See supplementary material at http://dx.doi.org/10.1063/1.4936613 for additional details on sample preparation and characterization.
[18]P. Pyykkö and M. Atsumi, Chem. - Eur. J. **15**, 186 (2009).
[19]S. Major, A. Banerjee, and K. L. Chopra, J. Mater. Res. **1**, 300 (1986).
[20]M. H. Yoon, S. H. Lee, H. L. Park, H. K. Kim, and M. S. Jang, J. Mater. Sci. Lett. **21**, 1703 (2002).
[21]P. P. Edwards, A. Porch, M. O. Jones, D. V. Morgan, and R. M. Perks, Dalton Trans. **19**, 2995 (2004).
[22]A. Janotti and C. G. Van de Walle, Rep. Prog. Phys. **72**, 126501 (2009).
[23]R. Saniz, Y. Xu, M. Matsubara, M. N. Amini, H. Dixit, D. Lamoen, and B. Partoens, J. Phys. Chem. Solids **74**, 45 (2013).
[24]M. Bazzani, A. Neroni, A. Calzolari, and A. Catellani, Appl. Phys. Lett. **98**, 121907 (2011).
[25]T. Kemmitt, B. Ingham, and R. Linklater, J. Phys. Chem. C **115**, 15031 (2011).
[26]J. R. Bellingham, W. A. Phillips, and C. J. Adkins, J. Mater. Sci. Lett. **11**, 263 (1992).
[27]R. Wang, A. W. Sleight, R. Platzer, and J. A. Gardner, J. Solid State Chem. **122**, 166 (1996).
[28]T. K. Gupta, J. Am. Ceram. Soc. **73**, 1817 (1990).
[29]K. Ellmer and R. Mientus, Thin Solid Films **516**, 4620 (2008).
[30]A. T. Vai, V. L. Kuznetsov, J. R. Dilworth, and P. P. Edwards, J. Mater. Chem. C **2**, 9643 (2014).
[31]R. Einzinger, in *Grain Boundaries in Semiconductors*, edited by H. J. Leamy, G. E. Pike, and C. H. Seager (Elsevier, New York, 1982), pp. 343–355.
[32]J. Y. W. Seto, J. Appl. Phys. **46**, 5247 (1975).
[33]J. W. Orton and M. J. Powell, Rep. Prog. Phys. **43**, 1263 (1980).
[34]M. W. J. Prins, K. O. Grosse-Holz, J. F. M. Cillessen, and L. F. Feiner, J. Appl. Phys. **83**, 888 (1998).
[35]K. Ellmer, in *Transparent Conductive Zinc Oxide: Basics and Applications in Thin Film Solar Cells*, edited by K. Ellmer, A. Klein, and B. Rech (Springer-Verlag, Berlin, 2008), pp. 35–78.
[36]J. D. Zook, Phys. Rev. **136**, A869 (1964).
[37]J. Jerhot and V. Šnejdar, Thin Solid Films **52**, 379 (1978).